THE ASTROPHYSICAL JOURNAL, 254:437–450, 1982 March 15

A SURVEY OF GALAXY REDSHIFTS. III. THE DENSITY FIELD AND THE INDUCED GRAVITY FIELD

MARC DAVIS AND JOHN HUCHRA
Harvard-Smithsonian Center for Astrophysics
Received 1981 June 26; accepted 1981 October 2

ABSTRACT

We have recently completed a redshift survey of galaxies complete to 14.5 m_Z in the north and south galactic polar caps containing some 2400 objects. Using an estimator unbiased by the known inhomogeneity of matter, we here compute the number density and luminosity density of bright galaxies to a distance of 80 Mpc ($H_0 = 100$) over the 2.7 sr of the survey. A plot of density versus distance vividly demonstrates the existence of a region 30 Mpc in extent beyond the Virgo cluster that is underdense by nearly a factor of 2 from the mean. However, averaging over the full sample volume of 4×10^5 Mpc^3, the number density and luminosity density given in the north and south catalogs agree to within 7%, suggesting that the survey is perhaps approaching a fair sample volume of the universe. The mean overdensity $\bar{\delta}$ toward the Virgo cluster is measured to be 2.0 ± 0.2, an important number for Virgocentric estimates of Ω. Finally, we examine the local peculiar gravity $\boldsymbol{g}$ induced by the inhomogeneous distribution of matter at large distances, assuming mass density to be at least approximately distributed as the large-scale number density of galaxies. In the limit of linear perturbation theory, $\boldsymbol{g}$ is proportional to the expected peculiar motion of the local group $\boldsymbol{v}_p$, for which we derive $|\boldsymbol{v}_p| \sim 670\ \Omega^{0.6}$, directed roughly toward the Virgo cluster. The assumptions of this cosmological test are quite different from the nonlinear, spherically symmetric Virgo infall test, and yet they both yield estimates of Ω that are quite high, $0.4 < \Omega < 0.5$, for an adopted infall velocity of 400 km s^{-1}. If the infall is as high as 500 km s^{-1}, the universe could very well be closed. However, if the infall is only 300 km s^{-1}, Ω is roughly one-third of the closure density.

Subject headings: cosmology — galaxies: clusters of — galaxies: redshifts

I. INTRODUCTION

For the past 3 years, we have engaged in a large-scale redshift survey of galaxies, which is now virtually 100% complete and contains approximately 2400 objects. Our sample is based on the Zwicky *et al.* (1968) catalog to a limiting Zwicky magnitude of 14.5. The sample boundary is ($\delta \geq 0$, $b \geq 40$) in the north galactic cap, and ($\delta \geq -2.5$, $b \leq -30$) in the south galactic cap, which is a solid angle of 1.83 sr in the north and 0.83 sr in the south. Various projections of the resulting redshift space maps for this sample are given by Davis *et al.* (1981, hereafter DHLT, Paper II of this series). This sample reaches far beyond the local Virgo supercluster and appears to have some statistical uniformity between the north and south, as evidenced from the similar distributions of the redshift space maps. Our redshift catalogs are in preparation and will be published elsewhere.

This is the first wide-angle sample not dominated by the Local supercluster, and it surveys a volume of space approximately 3.5 times larger than the Shapley-Ames catalog. We believe that the 14.5 sample is beginning to survey a sufficiently large volume to define a "fair sample" of the universe. In this paper, we study the luminosity and number density of galaxies and compare our results to previous studies. Yahil, Sandage, and Tammann (1980, hereafter YST) have presented a similar analysis for the Shapley-Ames sample, and Felten (1977) summarizes previous work based primarily on de Vaucouleurs *et al.* (1976). Kirshner, Oemler, and Schechter (1979, hereafter KOS), have used techniques similar to those described here in their study of the luminosity function of selected regions surveyed to 15.5 mag.

Because of the size of our sample, we can afford to delete intrinsically faint objects to obtain a sample that is at least partially volume limited and less affected by the severe local inhomogeneity of the Virgo supercluster. We observe that the luminosity function is fairly sensitive to the assumed Virgocentric flow model and that a measure of the flow can be obtained if the luminosity function is required to match between the northern and southern samples. For these intrinsically luminous galaxies, we derive a luminosity function unbiased by the presence of large inhomogeneities and compute their luminosity and number density in an unbiased fashion.

In § II, we display the observed luminosity distribution function for the north and south samples, finding them to be quite similar and moderately well fitted by a Schechter luminosity function. For this paper's purposes, we do not depend on this specific analytic form but rather describe a more general parameterization of the luminosity function well suited for the unbiased estimators.

In § III, the determined luminosity function is used to compare a plot of the observed velocity distribution of our sample with what would be expected in a homogeneous universe. Here one can vividly see the presence of a large hole behind the foreground Virgo cluster. Perhaps surprisingly, however, the average number and luminosity density for the north and for the south agree remarkably well. We also derive in this section the average overdensity of the Virgo supercluster interior to the radius of the Local Group of galaxies.

Given a luminosity function and radial shell counts, one can also derive, using linear perturbation theory, the peculiar gravity caused by the inhomogeneous matter distribution on large scales and the expected velocity of the Local Group of galaxies. This technique and its underlying assumptions are discussed in § IV. The results of this cosmological test are discussed in § V, and our general conclusions are summarized in § VI.

II. THE LUMINOSITY FUNCTION

A serious problem for traditional methods of luminosity function determination is the effect of large spatial inhomogeneities in the selected sample. If, for example, there is a large cluster (hole) occupying the foreground of the solid angle surveyed, there will be an overabundance (underabundance) of faint galaxies counted. For a homogeneous distribution, if $N(M)\,dM$ galaxies are counted in a magnitude interval dM, then the differential luminosity density $\Phi(M)\,dM$ is

$$\Phi(M)\,dM = N(M)\,dM/\left(\varpi D_M^3/3\right),$$

$$D_M = 10^{0.2(m_L - M)+1}\ \text{pc}, \qquad (1)$$

where m_L is the magnitude limit of the survey and ϖ is the solid angle surveyed. This relationship assumes that $\Phi(M)$ is a universal function independent of distance, clustering environment of the objects, and so forth. One is also required to assume that a simple relationship exists between magnitude and distance of each object.

In Figure 1, we plot the observed luminosity function $\Phi(M)$ defined as in equation (1) for the northern and southern samples of our survey. We assume no infall correction to the Virgo supercluster and use velocity as a distance estimator, using pure Hubble flow ($H_0 = 100$ km s^{-1} Mpc^{-1}) for each object after correcting for 300 km s^{-1} galactic rotation. Galaxies within 6° of the center of the Virgo cluster and with measured velocities

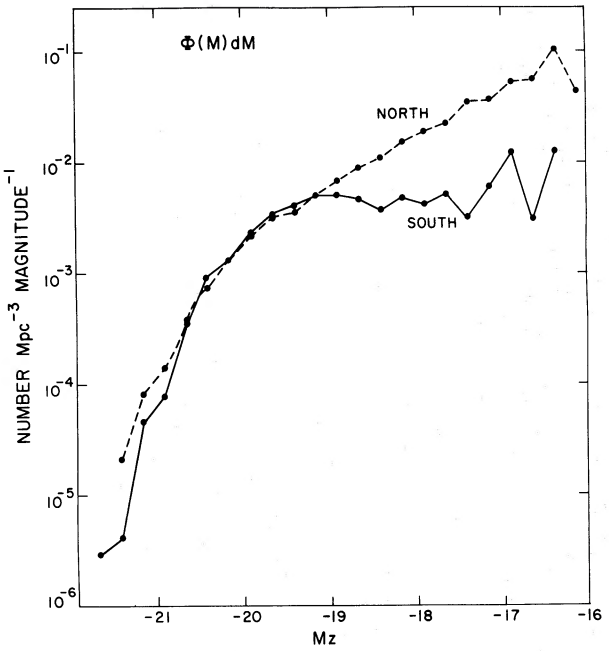

FIG. 1.—The observed differential luminosity function $\Phi(M)$ of the full north and south catalogs. No Virgocentric infall is assumed and only objects with $M < -16.0$ are plotted. The substantial excess of low-luminosity galaxies in the north is the result of the Virgo overdensity.

less than 2500 km s^{-1} are assumed to be at the mean Virgo velocity, 1020 km s^{-1} (Mould, Aaronson, and Huchra 1980). We have used Zwicky magnitudes and have made no correction for galactic extinction, which should be acceptable for the high-latitude data ($|b| > 40$) but is obviously questionable for lower latitudes, especially in view of the patchy obscuration over a portion of the southern galactic sample (see the maps of DHLT). However, a plot of $\Phi(M)$ in the south that is limited to galaxies with $b \leq -40$ is virtually identical to Figure 1. Galactic extinction that is nearly constant over latitude will naturally affect the calculated M, but it is unimportant for our analysis and will be ignored. The reddening at the north galactic pole does seem to be negligible, but there is a possibility of some patchy extinction in the south galactic cap (Burstein and Heiles 1978). A differential extinction of as little as 0.2 mag between the north and south can seriously affect some of the analysis described below.

Note that the bright end of the luminosity function is very similar for the two samples, but the faint end is considerably steeper for the north. This is hardly surprising because the fainter objects in the north are all close enough to be part of the large Virgo supercluster, whereas the corresponding volume in the south is largely devoid of all galaxies. Thus, it is apparent that the extrapolation of $\Phi(M)$ to faint magnitudes is subject to considerable bias.

TABLE 1

LUMINOSITY FUNCTION PARAMETERS

Sample	Virgo Infall	N_{GAL}	α	M^*	$\phi^* \times 10^{-3}$
North	0	1846	−1.6	−19.5	11
South	0	550	−0.6	−19.0	17
All	0	2396	−1.5	−19.5	11
All	300	2396	−1.3	−19.4	14
All	440	2396	−1.3	−19.4	13
All–E+S0	440	835	−1.1	−19.4	5
All–S+IRR	440	1560	−1.3	−19.3	9
Shapley-Ames $\|b\|>30$	440	1094	−1.0	−19.1	27
Shapley-Ames $b<-30$	440	344	−1.3	−19.3	12

The function $\Phi(M)$ is not separated here into different morphological types, a question which will be dealt with in a future paper. Table 1 does list the fit to Schechter function parameters for different morphological classes, as described below. We comment only that the luminosity distributions are again remarkably similar across morphologies; the major distinction is again the faint end of $\Phi(M)$ for the north versus the south.

It is relatively straightforward to make Virgocentric flow corrections to the velocity of each galaxy using the procedure described in DHLT and in Tonry and Davis (1981). These models assume a Virgocentric infall velocity field varying inversely as the Virgocentric distance and presume the mean redshift of the Virgo cluster to be 1020 km s^{-1}. The models are therefore uniquely scaled by the assumed Virgocentric infall of the Local Group of galaxies. The $\Phi(M)$ derived after an infall correction of 440 km s^{-1} for the Local Group is not noticeably changed from Figure 1 except at the faint end of the northern sample, which is made slightly shallower.

The observed $\Phi(M)$ can be fit to a Schechter (1976) luminosity function:

$$\Phi(L)\,dL = \Phi_*\left(L/L_*\right)^{\alpha} \exp\left(-L/L_*\right) dL. \quad (2)$$

This function is analytically convenient and is moderately accurate, although by no means does it give a precise fit to the observed $\Phi(M)$. In particular, it is difficult to fit simultaneously a flat slope at the faint end and a steep cutoff at the bright end. In Table 1, we list values of α and L_*, as determined in this way for our sample selected by morphological classes as listed by Nilson (1973). Elliptical and S0 galaxies are lumped together, as are spiral and irregular galaxies both for the north and south samples, with zero Virgocentric infall assumed. All morphological types are then binned together for various infall velocities to test the sensitivity. Again, because the fits are quite heavily affected by the weighting of the faint and bright ends, one should exercise caution in the interpretation of Table 1. Also beware of the −90% covariance between α, Φ^*, and L^*. A good working approximation is $\alpha = -1.3$ and $M_* = -19.4$, values quite consistent with those derived by Gott and Turner (1976) and other workers. A more complete discussion of Φ will follow in a later paper.

In view of the possibilities for bias in the determination of $\Phi(M)$, for the following analysis we have chosen to determine the luminosity function and selection function via a method described by Turner (1979) and used by KOS and Davis *et al.* (1980, hereafter DTHL) that is unbiased by density inhomogeneity. In turn, this method sacrifices knowledge of the overall scaling of Φ (Φ_*) in equation (2), which must be determined separately.

The basis of this technique is the commonly used assumption that the luminosity of a galaxy is a random variable uncorrelated with its position or environment. This assumption cannot be strictly true because the morphology of a galaxy is definitely a function of its environment and the luminosity functions of the different morphological types are similar but not identical. It is, however, a very good approximation, as shown vividly in the intercomparison of Figures 2*a* and 2*d* of DHLT for the nearby northern field, where both the bright and the faint galaxies define the clustering equally well. A plot of absolute luminosity versus local space density for all the bright objects in our northern sample is a complete scatter plot showing no correlation whatsoever. In addition, the fitted Schechter function parameters for the early-type versus late-type galaxies are virtually identical (see Table 1).

Define the selection function, $\phi(r)$, to be the fraction of objects at distance r that have been included in the catalog because they are observable to a distance r or greater (i.e., those objects with apparent magnitude equal to or less than the catalog limit). Suppose that $T(r)$ galaxies observed within a distance r are observable to distances $\geq r$ and suppose there are $F(r)$ observed galaxies whose maximum observable distance is within r and $r+\Delta r$. Then, if the luminosity of a galaxy were indeed a random variable, one would expect, independent of inhomogeneities, that the fractional change of

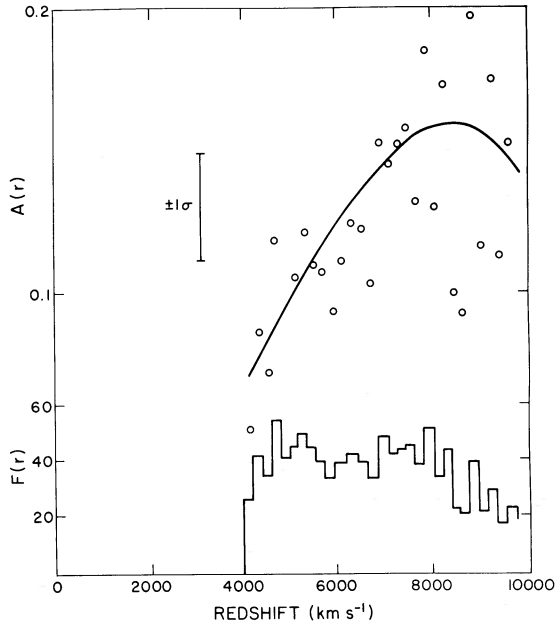

FIG. 2.—$A(r)$ and $F(r)$ as measured for the northern sample assuming Virgocentric infall of 440 km s^{-1}. The smooth curve is the polynomial fit to $A(r)$. The error bar is a typical $\pm\sigma$ error of the points defining $A(r)$ as expected from Poisson fluctuations.

$\phi(r)$ would be given by the ratio of $F(r)$ and $T(r)$, i.e.,

$$\frac{\phi(r+\Delta r)-\phi(r)}{\phi(r)} \approx \frac{d}{dr}[\ln \phi(r)]\,\Delta r = \frac{-F(r)}{T(r)} \equiv -A(r). \quad (3)$$

This relation presumes the catalog is complete to its limiting magnitude and that no differential extinction corrections are required. KOS binned their data into equal luminosity intervals and then fitted Schechter parameters to the resulting $A(L)$. We instead bin the data in equal distance intervals [$\Delta r \propto (\Delta L^{1/2})$] because this spreads the data more uniformly rather than clumping the bulk of the objects into only a few increments. We also find $\phi(r)$ to be a more convenient form for the considerations discussed below. The data is binned in redshift windows of 200 km s^{-1} shells between 0 and 10,000 km s^{-1}, and galaxies with corrected velocity outside this range are deleted. Equation (3) can of course be integrated directly, but, to reduce the effects of random statistical error, we fit $A(r)$ to a fourth-order polynomial and then analytically integrate it to find $\phi(r)$. This yields a five-parameter fit to $\phi(r)$ rather than the two parameters of the Schechter function, and, since we have no *a priori* knowledge of the analytic form of $\phi(r)$, our method is quite general. As a comparison check to the Schechter luminosity function, this procedure was applied with redshift bins of 400 km s^{-1} and a maximum redshift of 20,000 km s^{-1} to samples of galaxies with absolute magnitude $M \leq -16.0$, and the resulting $\phi(r)$ was differentiated and then fitted against the Schechter function parameters α and L_*. The result for the north with no infall is $\alpha = -0.9$ and $M_* = -19.2$, substantially different from the values of Table 1 and demonstrating the necessity of correction for the spatial inhomogeneity.

It is important to compare the nearby Virgo cluster to a deeper environment of groups and Abell clusters, but, of course, the luminosity function has been sampled to much fainter levels in Virgo compared, for example, to Coma. Therefore, we have made a partially volume-limited catalog by deleting objects that are not observable to a distance of at least 4000 km s^{-1} ($M_Z > -18.5$), considerably beyond the Virgo supercluster. This typically deletes one-third of the sample galaxies but results in a $\phi(r)$ with much less decrease from foreground to background, and therefore in considerably improved statistics. The resulting $\phi(r)$ is a very detailed fit to the luminosity distribution function between absolute magnitudes -18.5 to -20.5, roughly 1 mag either side of M_*.

As a typical example, Figure 2 plots $A(r)$ and $F(r)$ for the northern sample assuming the Virgo infall for the Local Group to be 440 km s^{-1}. The error bars shown are based on the typical Poisson fluctuations in the numerator and do not include the additional correlated fluctuations induced by $F(r)$ and $T(r)$. Also shown is the fit of the fourth-order polynomial to $A(r)$, which seems quite adequate, although is unnecessary for this data set. With the prescribed selection procedures, 1230 objects remain in the sample from an original list of 1846 galaxies. The $\phi(r)$ so determined is plotted in Figure 3 for the north and south catalogs, with and without correction for Virgocentric infall. To increase the sample size, the full southern sample is used, although the $\phi(r)$ changes only slightly if the catalog is limited to $|b| > 40$. Because the infall affects the southern sample only slightly, its $\phi(r)$ is plotted only once.

By definition, $\phi(r) = 1$ for $r \leq 40$ Mpc, and it falls quite steeply at large r. A characteristic point on the curve is the value of ϕ(80 Mpc), which is the fraction of objects with magnitude ≤ -20.0 and is typically 10%. Table 2 lists $\phi(80)$ plus the number of objects meeting the selection criteria for a variety of samples and with different infall velocities, as well as additional parameters to be discussed below.

As a test of the statistical accuracy of our procedure, we generated a series of catalogs of 300 randomly distributed points with luminosities randomly drawn from the $\phi(r)$ observed in the northern sample and then computed $\phi(r)$ for each catalog by the above procedure. We found no systematic bias in the measured $\phi(r)$ and determined the rms error of ϕ(80 Mpc) to be $\pm 17\%$. For a 1200 point sample, the expected statistical errors of

TABLE 2

DENSITY OF BRIGHT ($M < -18.5$) GALAXIES

Sample	$\|b\|$ Limit	Virgo Infall (km s^{-1})	Number	$\langle V/V_M \rangle$	$\phi(80)$	n_1 $\times 10^{-3}$ Mpc^{-3}	n_2 $\times 10^{-3}$ Mpc^{-3}	n_3 $\times 10^{-3}$ Mpc^{-3}	$\mathcal{L}_{BG}$ ($\times 10^7$ $L_\odot$/Mpc^{-3})
N-14.5	40	0	1016	0.50	0.053	11.4	12.3	8.3	7.8
N-14.5	40	220	1127	0.47	0.069	10.5	13.7	8.3	7.6
N-14.5	40	440	1230	0.45	0.095	9.0	13.1	8.2	6.8
S-14.5.....	40	0	284	0.54	0.061	8.2	7.9	8.2	5.7
S-14.5.....	30	0	455	0.56	0.078	7.4	6.7	7.4	5.4
S-14.5.....	40	440	275	0.55	0.057	8.5	8.2	8.5	5.7
S-14.5.....	30	440	444	0.56	0.075	7.6	7.0	7.6	5.4
S-13.0.....	40	0	157	0.40	0.092[a]	4.5	7.4	6.6	3.6
S-13.0.....	40	440	146	0.40	0.062[a]	6.0	8.5	7.3	4.4
Simulation: 14.5	40	0	1017	0.52	0.12	6.2	6.1	6.2	5.0

[a] ϕ (40 Mpc).

$\phi(80$ Mpc) should be less than 10%, and the larger fluctuations shown in Figure 3 and Table 2 must arise from systematic effects.

It is most interesting that $\phi(r)$ is sensitive to the assumed infall, especially in the north, but it is not unexpected. Local motion affects only slightly the most distant objects but results in substantial shearing of the Virgo region, making all the Virgo core galaxies more luminous for larger infall. If one conjectures that all is well with the magnitudes, then perhaps the Local Group infall to Virgo can be measured by insisting that $\phi(r)$ for the northern and southern samples match as well as possible. Of course, this is the basis of the measurement of the infall by YST for the revised Shapley-Ames sample, and their most recent infall velocity estimate is 275 ± 75 km s^{-1} (Yahil 1982). From Figure 3, we can see that the $\phi(r)$ would match best for an infall of roughly 200 km s^{-1}, with an error of ~ 100 km s^{-1}.

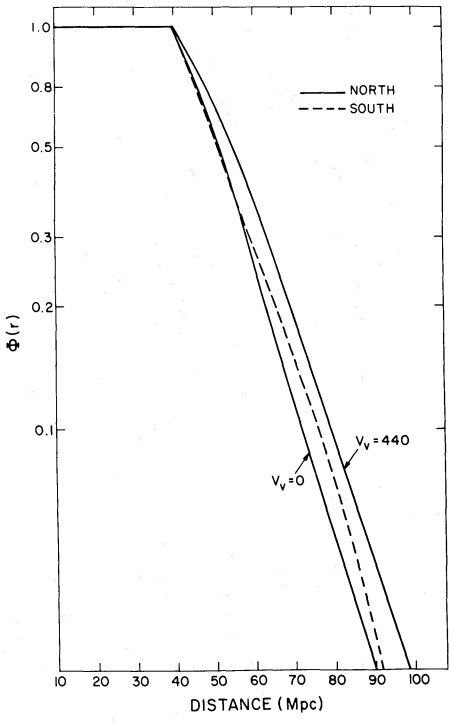

FIG. 3.—$\phi(r)$ for the north assuming infall of 0 and 440 km s^{-1}. The dashed line is $\phi(r)$ for the full southern sample assuming a Virgocentric infall of 440 km s^{-1}. Note that this curve will not precisely match the north for any value of Virgocentric flow.

Our result must be taken with a large grain of salt however. It is totally dependent on the Zwicky magnitude system, for which there are possible systematic errors in Volume 1 (Huchra 1981). There has been little checking of the Zwicky magnitudes in the south galactic cap, or for magnitudes fainter than $m = 14.0$ mag. Systematic magnitude errors will obviously completely bias the results of the above analysis and must be carefully investigated before the results can be trusted. If there is galactic absorption at the poles differing by as little as 0.2 mag between the north and the south, the analysis again will be seriously biased. The shapes of the selection functions are somewhat different in the north and the south, and no Virgocentric infall correction can match them precisely. Whether this is due to systematic photometry errors or is a real fluctuation in the luminosity distribution is unknown. In the next section, we show that the number density and luminosity density of the north and the south agree fairly closely, perhaps suggesting that the Zwicky magnitude system is not seriously in error. It would obviously be worthwhile to improve the photometry of our sample, or at least to check further the statistical and systematic errors of the Zwicky magnitudes.

III. THE DENSITY FIELD

a) The Space Density of Bright Galaxies

If space were homogeneous, the number of galaxies $N(r)$ observed in a shell of thickness Δr would be

$$N(r)=\varpi n r^2 \phi(r)\Delta r, \qquad (4)$$

where ϖ is the relevant solid angle and n is the space number density of galaxies. In Figure 4, for the Efstathiou and Eastwood (1981) n-body simulation discussed in DHLT, we plot the observed radial distribution of points, as well as the function $r^2\phi(r)$ as determined for this catalog. The curves are seen to match quite well, so the clustering of the simulation does not affect the overall homogeneity of the sample, and the measured value of $\langle V/M_m\rangle=0.52$, consistent with the value of $0.5\pm 1/12N^{1/2}$ expected for a complete, homogeneous, randomly distributed data set (Schmidt 1968). A measure of the mean density of a radial shell is the ratio of the observed to the predicted radial distribution, and this is shown as the dotted curve in Figure 4. Here, the clustering causes fluctuations larger than expected from a random Poisson distribution, but there is no trend with distance, which implies that our method of determination of $\phi(r)$ is unbiased. Similar tests with the randomly distributed data sets confirm this result.

In the real universe the situation is not quite so simple. Figures 5*a* and 6 plot the observed radial distribution and measured $r^2\phi(r)$ for the north and south samples, with an assumed Virgo infall of 440 km s^{-1}. Figure 5*b* shows the same plots in the north with no Virgo infall assumed. In each case, the dotted line is again the ratio of the observed to the predicted shell counts. In contrast to the simulation, here we see enormous fluctuations.

The Virgo supercluster looms over practically the entire northern sky in the foreground, and so it produces a large overdensity. On the other hand, the Coma/A1367 supercluster occupies only a fraction of the surveyed solid angle, and the overdensity at 6000–8000 km s^{-1} is not as pronounced in Figures 5*a* and 5*b*. The region of 3000–6000 km s^{-1} is of quite low density, in comparison. In the northern sample, as shown in Figure 5*a*, $\langle V/V_M\rangle=0.45$, so the large-scale inhomogeneities are quite significant, as is obvious. In the southern sample, shown in Figure 6, $\langle V/V_M\rangle=0.55$, and the prominent clustering is quite strongly concentrated at 5500 km s^{-1}, the same as the redshift of the Perseus chain of clusters which is separated from the bulk of the sample by some 20°–30° in the sky. With no assumed Virgo infall, the southern density profile is virtually unaffected. But, in the north, the Virgo overdensity is decreased, and the more distant overdensity is very substantially increased, as evident in Figure 5*b*, because $\phi(80)$ is a factor of 2 smaller. The trend of

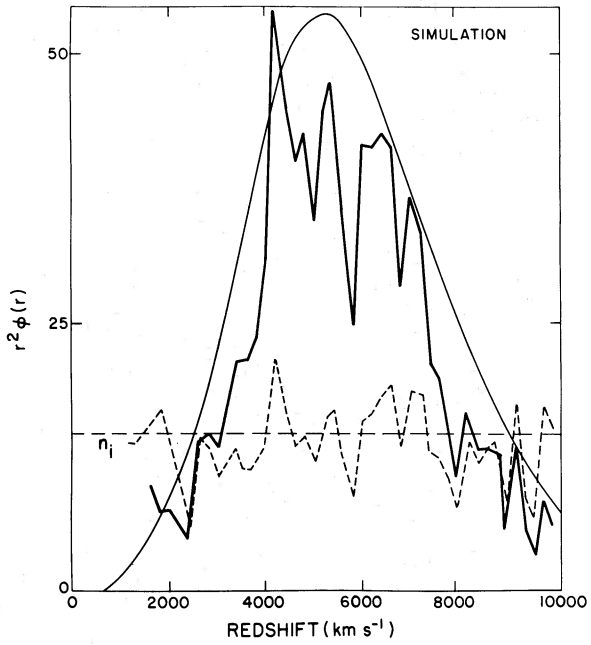

FIG. 4.—The solid heavy curve is the observed count of objects per radial shell of thickness 200 km s^{-1}, and the scale on the ordinate refers to this curve. This distribution results from the n-body simulation of Efstathiou and Eastwood (1981) as prepared by DHLT. The light curve is the distribution expected in a homogeneous (unclustered) universe, and the dashed curve is the ratio of the two. The scaling of these curves is arbitrary. The horizontal line is the value of n_1 as determined for this sample.

sharply increasing overdensity at large distance is almost surely the unphysical result of an improper selection function and demonstrates that inclusion of the Virgo flow correction is quite important.

In view of the large inhomogeneities, how is one to determine an unbiased estimate of the mean number density n of bright galaxies? There are at least three methods that come to mind, which offer varying degrees of bias versus stability and which we shall consider in turn.

Presuming $\phi(r)$ is an unbiased estimator, if $N(r)$ galaxies are luminous enough to be counted on a shell at radius r, then $N(r)/\phi(r)$ is the unbiased estimate of the total expected number of galaxies present on this shell. Then, within a surveyed volume V, an unbiased estimate of the number density, which we label n_1, is

$$n_1=\frac{\int (N(r)/\phi(r))\,dr}{\int dV}. \qquad (5)$$

This procedure is perhaps unbiased, but it heavily weights the most distant points where $\phi(r)$ becomes small and less certain. We therefore cut off this integral

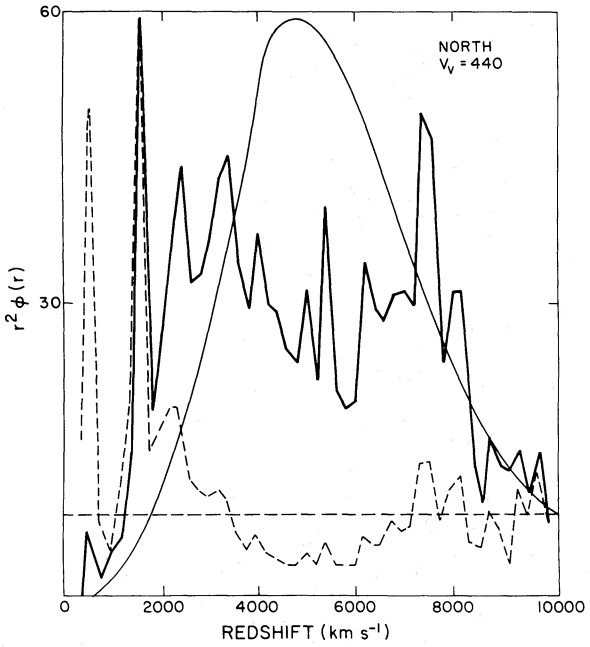

FIG. 5*a*

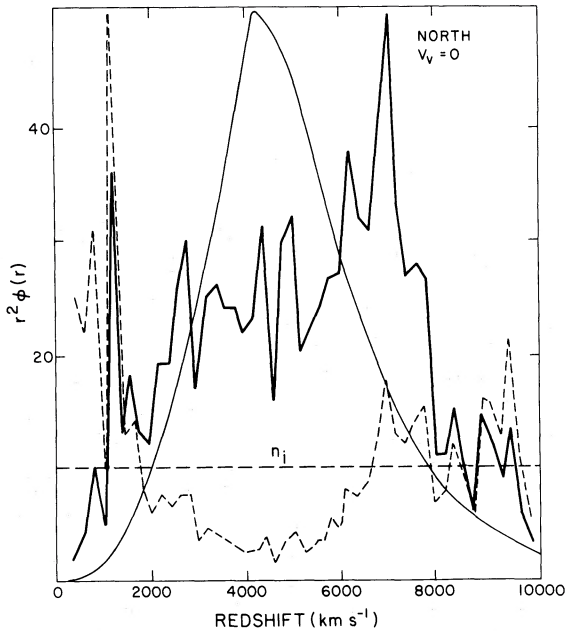

FIG. 5*b*

FIG. 5.—The same as Fig. 4, now for the northern sample of bright ($M \leq -18.5$) galaxies: (*a*) assuming Virgocentric infall of 440 km s^{-1}; (*b*) assuming no Virgocentric infall. Note how the Virgo supercluster dominates the foreground and how the relative contrast of the fluctuations changes between (*a*) and (*b*).

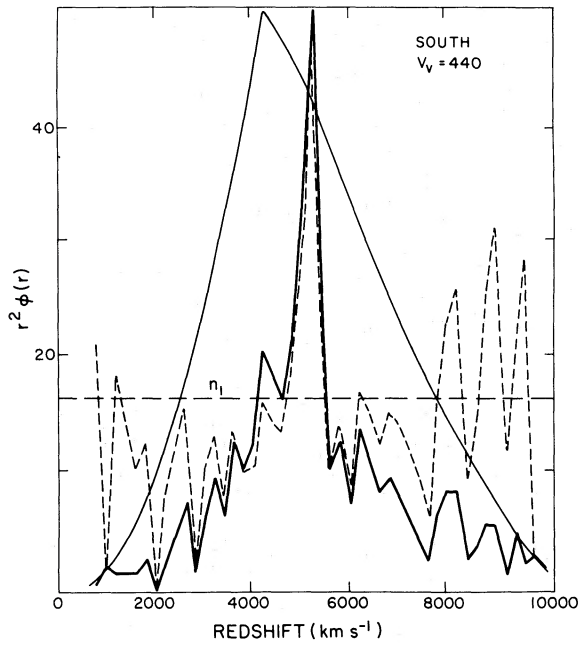

FIG. 6.—The same as Fig. 5 for the full southern sample of bright ($M < -18.5$) galaxies.

at a distance of 80 Mpc where $\phi(r) \sim 0.1$, a distance large enough to include the most prominent clusters, and about as far as one would dare correct for the selection function. In the Appendix we show that this is approximately the correct prescription to produce the minimum variance estimate of n and that the expected precision of our determination of n can be no better than 10%.

A much more stable estimate, but one that would be seriously affected by large-scale inhomogeneity in the foreground, is to compare the total number of counted objects N_T with what would be expected in a homogeneous universe. Call this estimator n_3, defined as

$$n_3 = N_T / \int \phi(r)\, dV. \tag{6}$$

Because all observed galaxies are weighted equally and there is no division by small numbers, this estimator is quite stable and relatively insensitive to changes in $\phi(r)$. This is also an unbiased estimator if there is no *a priori* knowledge of large-scale inhomogeneity in the sample. If $\langle V/V_m \rangle < 0.5$, we could expect n_3 to be an overestimate of the true density, and vice versa.

As an intermediate estimator, one can also average the density across radial shells to define an estimator n_2,

$$n_2 = \frac{\int N(r)/[r^2\phi(r)]\,dr}{\varpi \int dr}. \quad (7)$$

Here again, we cut off the integral at a radius of 80 Mpc. The estimator n_2 is also unbiased because it is the average of unbiased estimators, but its weighting is far from the minimum variance weights; note that it would be the mean level of the dashed curve in Figures 4–6.

In a homogeneous universe, all three estimates n_1, n_2, and n_3 would be equal, and, in tests of randomly distributed data sets containing only 300 points, they are equal within 10%. Table 2 summarizes these estimates for the 14.5 northern and southern surveys, with various Virgocentric infall velocities, and for an equivalent of the Shapley-Ames southern sample, $b \leq -40$, to 13.0 mag, which is the limit of completeness presently available over the entire sky. The 1.5 mag difference between the Shapley-Ames and our 14.5 mag sample translates to a factor of 2 in distance, so all distances relevant to the determination of $\phi(r)$ and (n_1, n_2) have been scaled down by this factor. In addition, we list in Table 2 the tabulated estimates for the n-body simulation discussed by DHLT, and here we see that the density estimates are quite consistent, within 2%, largely because this sample is so much more spatially homogeneous.

In Figures 4, 5, and 6, the dotted horizontal line is n_1 determined for each sample which serves to normalize the shell density fluctuations. Note in Figures 5*a* and 5*b* that the nearby shells dominated by Virgo have a density several times the mean, whereas the entire region between 3000 and 6000 km s^{-1} is only half the mean density. Also note that n_1 for the north and south samples agree remarkably well (within 7%) for an assumed infall of 440 km s^{-1} (see Table 2), but that the density of the shallow 13.0 mag southern sample is considerably lower. Thus, there are "holes" of lower than average density on both sides of the Virgo supercluster, but the overall density as seen within the 14.5 sample volume is perhaps reaching an asymptotic behavior. Again we caution that we have no assurance that all is well with the Zwicky magnitudes used here, and our results will of course be influenced by systematic errors. The lower density seen in the south $|b| > 30°$ sample is at least partly due to the patchy obscuration at the lower latitude for which no correction has been made.

Note from Table 2 that, as the Virgocentric infall is increased, very little occurs in the southern samples. But, in the northern sample, the number of selected galaxies increases, and yet the density estimate n_1 decreases, while n_3 remains stable and $\langle V/V_m \rangle$ decreases. This seemingly contradictory behavior is the result of increasing the absolute luminosity of the galaxies in the Virgo supercluster for increasing infall. The resulting $\phi(r)$ does not fall as rapidly for large infall; therefore, the overdensity of the distant northern shells is less, and these shells carry much of the weight in the determination of n_1. The $\langle V/V_m \rangle$ ratio is large for 0 infall because, then, few of the nearby Virgo galaxies are luminous enough to make the sample selection, and the total number of selected galaxies drops significantly. These effects are much smaller in the southern samples because there are no nearby large clusters and there is very little shearing of the velocity distribution. Also note that the estimate n_3 is very insensitive to the infall and agrees with the n_1 estimate in the north only for large infall values.

b) *The Luminosity Density of Bright Galaxies*

With the unbiased estimate of n and $\phi(r)$, we can compute directly the luminosity density of bright galaxies $\mathcal{L}_{BG}$ by

$$\mathcal{L}_{BG} = -n_1 \int \left[\frac{d\phi(r)}{dr}\right] L(r)\,dr, \quad (8)$$

where $L(r)$ is the luminosity of a galaxy whose limiting observable distance is r. This estimate is listed in Table 2 for each sample (in solar luminosities Mpc^{-3}). Since we have computed n only for galaxies in the absolute magnitude range $-18.5 > M > -20.5$, our estimate of luminosity density must be extrapolated to arrive at a total luminosity density. In § II, we found the Schechter function parameters $\alpha = -0.9$, $M_* = -19.2$ to be an approximate fit to the luminosity function between $-16 > M > -21$ after removing inhomogeneity effects. With these parameters, galaxies in the range $-18.5 > M > -20.5$ contribute 56% of the total light, so that the total luminosity density will be roughly a factor of 1.8 greater than the $\mathcal{L}_{BG}$ listed in Table 2. Again, this estimate is fairly uniform across the 14.5 mag samples, particularly for the larger infall estimates. Adopting a rough average $\mathcal{L}_{BG} = 6.5 \times 10^7\ \mathcal{L}_\odot$ Mpc^{-3} and total luminosity density $1.1 \times 10^8\ L_\odot$ Mpc^{-3}, the mean ratio of mass to luminosity in the universe is $M_\odot/L_\odot = 2350\ \Omega$, in good agreement with previous estimates (Davis, Geller, and Huchra 1978; Faber and Gallagher 1979, and references therein).

c) *The Mean Overdensity of the Virgo Supercluster*

Given a background density and an assumed Virgo flow model, we can readily compute the observed density of galaxies within the Virgocentric distance d_v of the Local Group of galaxies. The total number of the galaxies counted, the mean density $\bar{n}_v$ within this volume, and the mean overdensity $\bar{\delta} = \bar{n}_v/n_1 - 1$ are listed in Table 3 for several assumed values of the Virgo infall.

TABLE 3

VIRGO OVERDENSITY

Assumed Infall (km s^{-1})	Galaxies Counted Within d_v	Countable Fraction	$\bar{n}_v$ ($\times 10^{-2}$ Mpc^{-3})	$\bar{\delta}$	Ω
0	90	0.55	3.7	2.2	0
220	151	0.58	3.1	2.0	0.18
440	398	0.60	2.8	2.06	0.38

Each of these is derived from the partially volume-limited catalogs which are self-consistently generated for each infall velocity and use the appropriate n_1 from Table 2. In each case, the Virgo region is completely volume limited, so $\bar{n}_v$ should be quite reliable, and the systematic error in $\bar{\delta}$ is dominated by uncertainty in n_1. Because of the survey boundaries, we sample only about 60% of the Virgocentric sphere with radius equal to the distance of Local Group; this fraction depends somewhat on the assumed infall and is also listed in Table 3. The computed $\bar{\delta}$ presumes the density in the unsampled volume to be equal to the sampled volume, which is incorrect because of the central clumping of the Virgo core. It is known that the southern extension of the Virgo cluster is not as dense as the core, and therefore our estimates of $\bar{\delta}$ are a conservative upper limit. The results shown in Table 3 display some sensitivity to the assumed Virgo infall but not nearly as much as given by DTHL. The differences between the present result and that of DTHL are due to a catalog now 0.5 mag deeper, and the self-consistent determination of the background density in a volume that is large compared to the Virgo supercluster.

Our derived $\bar{\delta}$ is in the range $2<\bar{\delta}<2.2$ for all assumed values of the Virgo flow, so that there is little ambiguity in this number. We adopt $\bar{\delta}=2.0\pm0.2$, where the error is dominated by uncertainty in n_1. If the mean Virgo infall at distance d_v is 250 km s^{-1}, then the spherically symmetric, nonlinear models (DTHL) give $\Omega\sim0.2$, whereas, if the correct infall is 440 km s^{-1}, $\Omega\sim0.4$. The limitations of this type of model are discussed in § V*b*, but the results do agree with a simpler test to be discussed next.

IV. THE LOCAL GRAVITY FIELD

If one assumes that the mass distribution is correlated with the light distribution of the universe, at least in some large-scale overall way, then it is possible to compute the peculiar (non–Hubble) gravity $\boldsymbol{g}$ due to the observed inhomogeneity of the universe acting on our Local Group of galaxies. In the limit of linear perturbations dominated by the growing mode solution, a situation that should approximately apply for the infall of the Local Group to Virgo, the generated peculiar velocity $\boldsymbol{v}_p$ is simply related to $\boldsymbol{g}$ by (Peebles 1980, p. 64)

$$\boldsymbol{v}_p=\frac{2}{3}\frac{f}{H_0\Omega}\boldsymbol{g},\quad f\sim\Omega^{0.6}. \tag{9}$$

The local peculiar gravity is in turn

$$\boldsymbol{g}=G\rho_c\Omega\int dV\left[\frac{n_c(\boldsymbol{r})/\phi(r)-n_1}{n_1}\right]\frac{\boldsymbol{r}}{r^3}, \tag{10}$$

where $n_c(\boldsymbol{r})$ is the number of counted objects per volume element at position $\boldsymbol{r}$. The integrand is simply the unbiased estimate of the local density fluctuations, and the integral must be cut off at large r (80 Mpc) so as not to divide by a small number, producing large fluctuations. The presumption therefore is that the contribution to $\boldsymbol{g}$ is 0 outside of the solid angle of the survey or beyond the distance of the cutoff, although distant fluctuations will only produce a small tidal shear across the observed volume, which affects our conclusions only slightly if the observed velocity v_v is measured from the shear field within this *same* volume.

A more convenient form of equations (9) and (10) results if we define the projection over the observed solid angle $\boldsymbol{p}$ as

$$\boldsymbol{p}=\frac{1}{\varpi}\int d\Omega\frac{\boldsymbol{r}}{r}, \tag{11}$$

and the direction-weighted shell density as

$$\boldsymbol{n}(r_s)=\frac{1}{\varpi\phi(r_s)r_s^2\Delta r}\int d\Omega\sum_i\delta(\boldsymbol{r}_s-\boldsymbol{r}_i)\frac{\boldsymbol{r}_i}{r_s}, \tag{12}$$

where r_s is the radius of a given shell of thickness Δr, δ is the Dirac delta function, and the sum over i includes only objects within that shell. Since $H_0^2=(8\pi/3)G\rho_c$, we can reduce equations (8)–(11) to

$$\boldsymbol{v}_p=(H_0\Delta r)\Omega^{0.6}\left(\frac{\varpi}{4\pi}\right)\sum_{\text{shells}}\left(\frac{\boldsymbol{n}(r_s)}{n_1}-\boldsymbol{p}\right). \tag{13}$$

Thus, each shell contributes equally to the peculiar

gravity because the expected number of galaxies per shell varies as r_s^2, canceling the $1/r_s^2$ factor for each individual galaxy. It is convenient to define a Cartesian coordinate system with the z-axis along the north galactic pole, the x-axis directed along ($b=0°$, $l=0°$), and the y-axis along ($b=0$, $l=90°$), in which case the geometry of our northern sample is $\boldsymbol{p}=(-0.06,0.09,0.70)$. If we had full sky coverage $\boldsymbol{p}$ would have been equal to zero. Of course, since our sample is at high galactic latitude, only the v_{p_z} component can be meaningfully estimated, and, to improve this estimate, one should naturally include whatever southern sky data is available.

In Figure 7 is shown the cumulative estimate of v_{p_z} as successive shells are added from the 14.5 northern sample and from the 13.0 southern sample with $b \leq -40$. We have here corrected observed redshifts for a Virgocentric infall velocity of 440 km s^{-1} and use the n_1 as determined from the north for this infall (Table 2). Comparison of equations (7) and (12) shows that $\boldsymbol{n}(r_s)$ is a vector version of $n_2(r)$, which is plotted in Figure 5 and exhibits large fluctuations from average. As shown in Figure 7, we integrate to a distance of 80 Mpc in the north and 40 Mpc in the south. Note how the peculiar velocity first increases for shells of distances up to and beyond the Virgo cluster, then falls for the intermediate low-density shells, and finally increases again for the denser shells at the distance of the Coma supercluster. The positive fluctuation in the southern region at 15 Mpc is caused by the Fornax cluster, but, on the average, the south acts as a negative mass pushing us northward. If one can presume that the contribution from subsequent shells is negligible, then, from Figure 7, we have $v_{p_z} \approx 620\ \Omega^{0.6}$ km s^{-1}. Including the small transverse velocity (v_{px}, v_{py}) increases this number slightly. In Table 4, we list v_p as determined by the quadrature sum of its three components, as well as the computed direction, for different values of the assumed Virgocentric infall. All these estimates of v_p were derived using the appropriate values of n_1 and $\phi(r)$, and all include the contribution from the southern 13.0 mag sample. Assuming that v_p is the same as the assumed infall, we list the derived Ω. Here we see that v_p is fairly insensitive to the assumed infall, with slightly smaller infall v_p predicted for lower assumed Virgocentric flow. This results from the increase of n_1 and the decrease of the influence of the Virgo region for low values of Virgocentric flow. In fact, for no Virgo flow, the northern sky contributes only two-thirds the total v_{p_z}, and the hole in the south becomes more significant, acting as a strong negative mass concentration. The final two columns in Table 4 list the Ω derived for assumed infall velocity of 300 and 500 km s^{-1} for each computed v_p. Ellipses appear in columns for entries not close to being self-consistent.

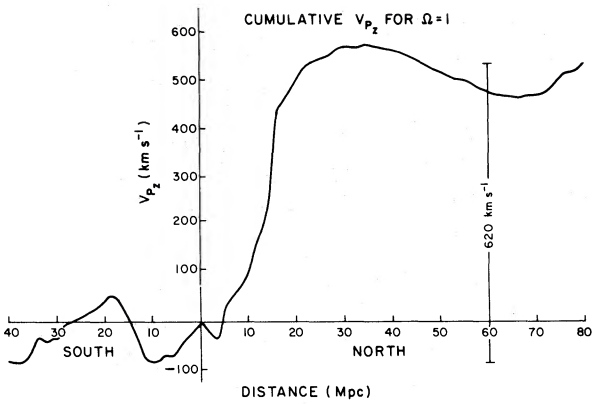

FIG. 7.—Cumulative estimates of v_{p_z} as successive shells are added to the calculation of $\boldsymbol{g}$. A Virgocentric infall of 440 km s^{-1} has been assumed in the computation of $\boldsymbol{g}$. The net velocity 620 $\Omega^{0.6}$ km s^{-1} results after integration to 80 Mpc in the north and 40 Mpc in the south.

It is interesting to note that the direction of pull is *not* toward the center of the Virgo cluster but rather toward $\sim 11^h.3$ and $+23°$. This is very close to the direction found from the sum of apparent luminosity vectors for al non–Local Group galaxies in the whole-sky Shapley-Ames sample: $11^h.9$ and $+26°$. In addition, both of these vectors are close to the microwave-background anisotropy vector (Smoot and Lubin 1979) *before* correction for galactic rotation: $11^h.4$ and $+10°$!

V. DISCUSSION

a) Comparison to Shapley-Ames

Our technique for determination of v_p is quite similar to a procedure described by YST who applied it to the

TABLE 4

PECULIAR GRAVITY RESULTS

Assumed Virgo Infall (km s^{-1})	$V_{p_z}\,\Omega^{0.6}$	$\lvert V_p\,\Omega^{0.6}\rvert$	Direction (α, δ)	Derived Ω	$v_v=300$ Ω	$v_v=500$ Ω
0	466	490	$11^h28^m, +21°$	0	...	...
220	529	571	11 12 , +23	0.2	0.34	...
440	620	670	11 08 , +24	0.5	0.26	0.61

revised Shapley-Ames catalog and arrived at $U_{LG} = 3800$ km s^{-1}. Their definition of U_{LG} is $3\Omega^{-0.6}$ times our definition of v_p, so there remains a difference of about a factor of 2 between these results which must be resolved.

The background density n, is critical for all these analyses. We have endeavored to define an unbiased average volume density which includes all the Abell clusters and holes within our sample. With the Shapley-Ames catalog, it is only possible to integrate to a distance of 40 Mpc, and YST determined a background density from the average of the southern and the northern regions outside of the Virgo region. They specifically excluded the Virgo region because they claimed it is too anomalous. However, as we see in Figure 5 and Table 2, the regions used for a background determination by YST are substantially underdense compared with the mean defined by the much larger, full northern volume. This difference substantially biases their estimates of U_{LG} and $\bar{\delta}$ to be high and explains their resulting low estimates of Ω. We are also subject to bias if we adopt an incorrect n, but, from the discussion in the Appendix, we believe the density is now known within 10%, barring systematic errors in the Zwicky magnitude system.

b) *The Virgocentric Flow*

Our estimate of the predicted v_p should be compared to the measured anisotropy of the Hubble flow resulting from a second distance indicator (de Vaucouleurs and Bollinger 1979; Aaronson *et al.* 1980; Tonry and Davis 1981), which suggests a Virgocentric infall v_v of 300–500 km s^{-1}. As seen from Figure 7, most of the expected velocity is induced by the Virgo cluster, although the hole in the southern sky contributes ~ 100 km s^{-1} repulsive velocity to the Local Group. Unfortunately, our information on v_x and v_y is too unreliable for a comparison to the velocity components indicated by the microwave background anisotropy (Smoot and Lubin 1979). Note, however, that the direction $\boldsymbol{v}_p$ is $\sim 25°$ away from the Virgo center and is deflected toward the nearby Leo, Canes Venatici, and Ursa Major groups, which is expected from the observed nonspherical distribution of the galaxies within the Virgo supercluster.

In the spherically symmetric Virgo flow models, the determined Ω is a sensitive function of $\bar{\delta}$. Our present analysis confirms the results of the DTHL work which was done on the 14.0 mag sample using a slightly different technique. Again, the derived value of Ω is in the range $0.2 < \Omega < 0.5$ for Virgocentric infall in the range $250 < v_v < 500$, a range that spans all recent work in this problem.

However, these spherically symmetric Virgo models are strictly applicable only for a number of assumptions which are not true in detail. They assume no subclustering of the Virgo region, whereas Virgo is far from spherically symmetric and subclustering could affect the infall estimate (Schechter 1980). The models assume the universe to be spherically symmetric outside the radius of the Local Group; this assumption is almost surely false in detail, although the effect of the substantial holes both in the south and in the north beyond Virgo will largely cancel. Perhaps the major difficulty, however, is knowing the mean redshift of the Virgo cluster in the presence of a non–Gaussian velocity distribution function and the possibility of substantial subclustering near the Virgo core. The Hubble flow anisotropy tests measure the distance to Virgo, so an increase in the assigned redshift of the Virgo center will result in an equal decrease in the computed Virgocentric flow (Yahil 1982), and this decreases the Ω estimate quite substantially. However, we cannot accept Yahil's suggestion that M87 ($v = 1180$ km s^{-1}), because of its extensive X-ray halo, must be at rest in the center of the potential well of the Virgo cluster. Recently, de Young, Condon, and Butcher (1980) showed that the morphology of Hα filaments to the north and extended radio emission to the south of M87 could only be understood as a bow shock induced by an approximately 100 km s^{-1} northward motion of M87 with respect to the intergalactic gas within the Virgo cluster. Given the existence of a transverse velocity of this magnitude, there is certainly no reason to deny the possibility of a comparable velocity in the redshift direction, and very likely the mean redshift of the Virgo cluster is 1020 km s^{-1}, as determined by the average of galaxies within the 6° core (Mould, Aaronson, and Huchra 1980).

The calculation of the peculiar gravity $\boldsymbol{g}$, on the other hand, is indifferent to the assumption of spherical symmetry and homogeneity and is insensitive to small (~ 100 km s^{-1}) errors in the mean redshift of the Virgo center. Its limiting factor is that $\boldsymbol{v}_p$ will be strictly proportional to $\boldsymbol{g}$ only in linear theory, whereas Virgo is a nonlinear fluctuation. If we adopt a measured infall toward the Virgo direction of 400 km s^{-1}, we derive $\Omega \sim 0.42$, and, if we correct for nonlinearities in the spherical model, we should adjust Ω upward to ~ 0.5, based on the behavior of spherically symmetric, nonlinear perturbations. Thus, this technique confirms the rather high Ω estimate derived by the exact, spherically symmetric models and yet is not nearly as model sensitive.

From Figure 7, we can see that the full amplitude of v_{p_z} is not reached for distances of less than 30 Mpc, so that measured infall velocities to Virgo based on the shear field of galaxies within this distance can be expected to be smaller than the Virgo flow velocity based on more distant reference points. At least part of the present disagreement on the proper Virgocentric velocity is likely to be caused by this effect. The studies using a reference frame of Abell clusters at 50–100 Mpc or elliptical galaxies at a comparable distance have yielded high estimates of the infall (~ 430–480 km s^{-1}) (Tonry and Davis 1981; Aaronson *et al.* 1980), while the studies

based on the Tully-Fisher-IR test for galaxies with $v <$ 3000 km s^{-1} (Schechter 1980) or based on magnitudes alone for the revised Shapley-Ames catalog (YST; Yahil 1982) have resulted in considerably lower estimates for the infall (200–300 km s^{-1}). Schechter's (1980) analysis is addressed to finding the mean infall velocity of galaxies at our Virgocentric distance and attempts specifically to remove the effects of subclustering to such nearby groups as the Leo cloud. This is not the desired velocity for comparison to $\boldsymbol{g}$ or $\boldsymbol{v}_p$ calculated above because the gravitational influence of subclustering of the various components of the Virgo supercluster has been included.

It is obviously important that these discrepancies be fully reconciled, but our inclination is that the results of Aaronson *et al.* (1980) and Tonry and Davis (1981) are most relevant for comparison to $\boldsymbol{v}_p$ because they have directly measured the velocity shear on a scale identical with our scale for the determination of $\boldsymbol{g}$. With an infall velocity of v_v of 500 km s^{-1}, the indicated Ω is 0.61, and, after correction for the nonlinearity of the flow, the implied Ω is 0.72, a number perilously close to 1. We estimate this value must be uncertain at the 20% level, so that a closed universe may be consistent with high infall estimates, but $\Omega < 0.1$ is not consistent with any current measure of the Virgocentric flow.

VI. SUMMARY AND CONCLUSIONS

We have presented density plots which vividly demonstrate the large-scale nature of the galaxy distribution to a distance of 100 Mpc ($H_0 = 100$). There are large "holes" behind Virgo and in the foreground of the southern sky which, combined with the large clusters, severely bias standard methods of determining luminosity functions and number densities. Our procedure for determining luminosity functions, selection functions, and mean densities is an attempt to minimize the bias induced by the large-scale inhomogeneities. It is apparent that observed velocities should be corrected for Virgocentric infall before an attempt is made to determine the luminosity function.

The derived mean densities of bright galaxies in our northern and southern samples agree remarkably well; this does not occur for 13.0 mag limited catalogs. Thus, we may, at limiting magnitude 14.5, finally be reaching toward a fair sample volume of the universe. This is obviously something that must be checked further, both by extending the survey to more of the southern sky and by either improving or, at least, checking the Zwicky magnitudes on which our conclusions depend.

By knowledge of the selection function of galaxies $\phi(r)$, we can derive the local peculiar (non–Hubble) gravity $\boldsymbol{g}$ from the observed space distribution of intrinsically bright galaxies. As expected, $\boldsymbol{g}$ is dominated by Virgo, but the numerous holes and more distant clusters make a substantial contribution, and the method does not depend on spherical symmetry for Virgo. It does, however, presume that no contribution to $\boldsymbol{g}$ occurs for regions outside the solid angle of the survey or at large distance (>80 Mpc in the north; >40 Mpc in the south). In linear perturbation theory, $\boldsymbol{g}$ is proportional to the induced peculiar velocity $\boldsymbol{v}_p$, and we find an expected $|\boldsymbol{v}_p| \sim 670\ \Omega^{0.6}$ km s^{-1}, directed within 25° of the Virgo core. However, the components of $\boldsymbol{v}_p$ directed along the galactic equator are very poorly determined, and only the component directed toward the galactic pole can be considered reliable. Fortunately, Virgo is itself at high latitude ($b \sim 79°$), and there are no known nearby clusters near the galactic plane of comparable magnitude.

Before interpreting $\boldsymbol{v}_p$ as a measurement of Ω, we must bear in mind several key assumptions:

1. The mass distribution of the universe is clustered in large scale like the bright galaxies; if for some reason the mass is less clumped than the light and the holes are not as empty as they appear, $\boldsymbol{g}$ and $\boldsymbol{v}_p$ will be overestimated and Ω underestimated.

2. There are no large clusters lurking just beyond our survey boundaries to confound our estimate of $\boldsymbol{g}$.

3. Any derived infall to Virgo is *generated* by the peculiar gravity field $\boldsymbol{g}$ and is not due to initial conditions since unsupported velocities adiabatically decay away in an expanding universe. However, in scenarios such as the coordinated supernovae model of Ostriker and Cowie (1981), large-scale motions are primarily hydrodynamically induced, and the formation epoch is comparatively recent ($z \sim 5$), so that substantial unsupported velocity could remain today and contribute at least partially to the measured Virgo infall.

4. The relationship between $\boldsymbol{g}$ and $\boldsymbol{v}_p$ applies only in the linear perturbation theory, whereas the Virgo supercluster has density contrast of $\bar{\delta} \sim 2$. However, the effect of nonlinearity is only to underestimate slightly the Ω estimate, provided that the system has not yet stopped expanding and begun to recollapse, an event quite far into the future for the Local Group and the Virgo supercluster.

With these assumptions in mind, Table 4 lists the derived cosmological density. For "reasonable" infall, $250 < v_v < 500$, the derived density estimate, after correction for nonlinearity of the flow, is $0.3 < \Omega < 0.7$, but the high-velocity and Ω estimates are preferred because they result from the largest scale measurements of the velocity shear field. The derived Ω estimates are quite consistent with the results of the nonlinear, spherically symmetric calculation (Table 3), so that the chief uncertainty in using Virgocentric infall as a cosmological probe is knowledge of the proper value of v_v. In the next few years there should be considerable progress on this problem.

It is clearly important to reexamine Ω determinations based on smaller scale sizes to understand whether the

present result is consistent with more traditional analyses based on virial equilibrium. Such an analysis has been done for the virialized groups of the present sample (Press and Davis 1982; Huchra and Geller 1982) with results that show a clear linear trend of the M/L ratio versus size of cluster. The Virgo infall results all fall below the extrapolation of the observed trend line and suggest that an asymptotic value of Ω is being approached on the scale of superclusters. However, until we understand the nature of the mysterious dark matter which so dominates the mass density of the universe and why it clusters only weakly with the luminous galaxies, we can only speculate inconclusively about which cosmological model applies to our little section of the universe.

This research was supported in part by NSF grant AST 80-00876. We thank Jim Felten for pointing out an error in an earlier version of this work.

APPENDIX

OPTIMAL WEIGHTING FUNCTION FOR DETERMINATION OF n

Suppose in a magnitude-limited survey that observed galaxies are distributed in cells, with n_i being the count of galaxies in cell i. If the cells are small, $n_i = 0$ or 1. Then, an unbiased estimator for the mean number density of galaxies $\bar{n}$ is

$$\bar{n} = \sum_i n_i w_i \Big/ \int dV \phi(r) w, \tag{A1}$$

where w is any weighting function we choose and $\phi(r)$ is the selection function. The expected variance of $\bar{n}$, $\langle \delta n^2 \rangle$, after averaging many independent data sets, is given by an integral over the galaxy covariance function $\xi(r)$ (Peebles 1980):

$$\langle n^2 \rangle = \frac{\sum w_i w_j \langle n_i n_j \rangle}{\left(\int dV \phi w \right)^2} = \frac{\bar{n}^2 \int dV_1 \, dV_2 w_1 w_2 \phi_1 \phi_2 \xi_{12} + \bar{n} \int dV w^2 \phi + \bar{n}^2}{\left(\int dV \phi w \right)^2}, \tag{A2}$$

$$\langle \delta n^2 \rangle = \langle n^2 \rangle - \langle \bar{n} \rangle^2 = \frac{\bar{n}^2 \int dV_1 \, dV_2 w_1 w_2 \phi_1 \phi_2 \xi_{12} + \bar{n} \int dV w^2 \phi}{\left(\int dV \phi w \right)^2}, \tag{A3}$$

$$= \frac{\bar{n}^2 J_3 \int dV w^2 \phi^2 + \bar{n} \int dV w^2 \phi}{\left(\int dV \phi w \right)^2}, \tag{A4}$$

where J_3 is the integral over the covariance function

$$J_3 = 4\pi \int_0^\infty r^2 \xi(r) \, dr \approx 3000\text{–}10{,}000 \text{ Mpc}^3.$$

Note that $nJ_3 \sim 30$–100 is the mean number of excess galaxies correlated about any random galaxy.

To minimize $\langle \delta n^2 \rangle$, set the derivative of equation (A4) with respect to w equal to 0, yielding

$$w(r) = \frac{1}{1 + \bar{n} J_3 \phi(r)} \sim \frac{1}{1 + 40\phi(r)}. \tag{A5}$$

Note that this is very close to the weighting used to determine n_1 in the text, where $w(r) = 1/[\phi(r)]$, $r < 80$ Mpc;

$w(r)=0$, $r>80$ Mpc. Equation (A5) suggests that the crossover point should occur for $\phi \approx 1/40$, which occurs generally at $r=100$ Mpc. This point is uncertain because J_3 is not known precisely, and our cutoff of 80 Mpc is slightly conservative. This analysis also does not include the uncertainty of $\phi(r)$ which is significant at large distance and prompts a conservative cutoff.

Given an optimal weighting w, we can evaluate equation (A4) to find

$$\langle \delta n^2 \rangle = \frac{\bar{n}}{\int dV \phi w},$$

or

$$\frac{\langle \delta n^2 \rangle^{1/2}}{\bar{n}} = \left(\frac{1}{\bar{n} \int dV \phi w} \right)^{1/2} \approx \left[\frac{J_3}{V} \right]^{1/2}.$$

The survey volume of our northern sample is 3×10^5 Mpc, so $\langle \delta n \rangle / n \sim 0.1$–$0.2$. This number is not surprising given the observed number of rich clusters in the surveyed volume. For the revised Shapley-Ames survey, however, the volume in which YST derived $\bar{n}$ is not more than 6×10^4 Mpc, and the minimum uncertainty of $\bar{n}$ is $\sim 30\%$, which is sufficient to explain the discrepancy between YST and the present results.

I thank Jim Peebles for suggesting this analysis of optimal weighting.

REFERENCES

Aaronson, M., Mould, J., Huchra, J., Sullivan, W. T., Schommer, P. H., and Bothun, G. D. 1980, *Ap. J.*, **239**, 12.
Burstein, D., and Heiles, C. 1978, *Ap. J.*, **225**, 40.
Davis, M., Geller, M., and Huchra, J. 1978, *Ap. J.*, **221**, 1.
Davis, M., Huchra, J., Latham, D. W., and Tonry, J. 1981, *Ap. J.*, **253**, 423 (DHLT).
Davis, M., Tonry, J., Huchra, J., and Latham, D. 1980, *Ap. J. (Letters)*, **238**, L113 (DTHL).
de Vaucouleurs, G., and Bollinger, G. 1979, *Ap. J.*, **233**, 433.
de Vaucouleurs, G., de Vaucouleurs, A., and Corwin, H. G. 1976, *Second Reference Catalogue of Bright Galaxies* (Austin: University of Texas).
de Young, D., Condon, J. J., and Butcher, H. 1980, *Ap. J.*, **242**, 511.
Efstathiou, G., and Eastwood, J. W., 1981, *M.N.R.A.S.*, **194**, 503.
Faber, S. M., and Gallagher, J. S. 1979, *Ann. Rev. Astr. Ap.*, **17**, 135.
Felten, J. E. 1977, *A.J.*, **82**, 861.
Gott, R., III, and Turner, E. L. 1976, *Ap. J.*, **209**, 1.
Huchra, J. 1981, private communication.
Huchra, J., and Geller, M. J. 1982, in preparation.
Kirshner, R., Oemler, A., and Schechter, P. 1979, *A.J.*, **84**, 951 (KOS).
Mould, J. M., Aaronson, M., and Huchra, J. 1980, *Ap. J.*, **238**, 458.
Nilson, P. 1973, *Uppsala General Catalogue of Galaxies*, *Uppsala Astr. Obs. Ann.*, Vol. **6**.
Ostriker, J. P., and Cowie, L. 1981, *Ap. J. (Letters)*, **243**, L127.
Peebles, P. J. F. 1980, *The Large-Scale Structure of the Universe* (Princeton: Princeton University Press).
Press, W. P., and Davis, M. 1982, *Ap. J.*, in press.
Schechter, P. 1976, *Ap. J.*, **203**, 297.
_____. 1980, private communication.
Schmidt, M. 1968, *Ap. J.*, **151**, 393.
Smoot, G. F., and Lubin, P. M. 1979, *Ap. J. (Letters)*, **234**, L83.
Tonry, J., and Davis, M. 1981, *Ap. J.*, **246**, 666.
Turner, E. 1979, *Ap. J.*, **231**, 645.
Yahil, A., Sandage, A., and Tammann, G. A. 1980, *Ap. J.*, **242**, 448 (YST).
Yahil, A. 1982, *Xth Texas Conference on Relativistic Astrophysics*, in press.
Zwicky, F., Herzog, E., Wild, P., Karpowicz, M., and Kowal, C., 1961–1968, *Catalog of Galaxies and of Clusters of Galaxies*, Vols. **1–6**, (Pasadena: California Institute of Technology).

MARC DAVIS: Department of Astronomy, University of California, Berkeley, CA 94702

JOHN HUCHRA: Center for Astrophysics, 60 Garden Street, Cambridge, MA 02138